EXPERIMENTAL INVESTIGATION ON AIRCRAFT DYNAMIC STABILITY PARAMETERS

FRANCESCO FUSCO[1] and GIORGIO GUGLIERI[2]

[1]*Centro Italiano Ricerche Aerospaziali, Via Maiorise, 81043 Capua, Italy.*

[2]*CNR Centro di Studio per la Dinamica dei Fluidi, Corso Duca degli Abruzzi 24, 10129 Torino, Italy.*

(Received: 26 November 1991; accepted in revised form: 15 October 1992)

ABSTRACT. In this paper, the design requirements of an experimental apparatus for the measurement of the direct derivatives on an oscillating aircraft model in a wind tunnel are discussed. The elaboration of the signal output of the force transducer is analysed, according to the direct forced oscillation technique. The distorsions of the primary oscillatory motion were previously evaluated and corrected, adopting an open loop control technique. This algorithm is presented and its reliability is verified. Finally, the behaviour of the experimental stability parameters, adopting different oscillation amplitudes and frequencies, is discussed.

SOMMARIO. Nel presente lavoro vengono analizzate le principali caratteristiche di un sistema per l'esecuzione delle prove di oscillazione forzata in galleria del vento, al fine di valutare le derivate aerodinamiche dirette, secondo i gradi di libertá alla rotazione di un velivolo. Inizialmente l'attenzione viene concentrata sul principio di funzionamento e sull'algoritmo di elaborazione dei segnali estensimetrici. L'analisi procede quindi con lo studio delle caratteristiche cinematiche del sistema di movimentazione e supporto, ed in particolare si discutono le problematiche connesse con il controllo del moto oscillatorio del modello. Infine, viene discusso l'utilizzo dell'apparecchiatura in oggetto con lo scopo di evidenziare come i parametri di stabilitá rilevati sperimentalmente dipendano dalle caratteristiche del moto armonico di forzamento.

KEY WORDS. Wind tunnel experiments, Aircraft dynamics.

1. INTRODUCTION

The experimental approach to the investigation of aircraft dynamics is widely diffused and many wind tunnel testing techniques were developed attempting to analyse the non-linearities which are typical for the flight envelopes of high-performance modern aircraft. As a consequence, these experimental data give the possibility of evaluating the aerodynamic loads acting on the airplane during some critical manoeuvres or flight conditions.

One of the methods, largely adopted for this kind of wind tunnel tests, is the direct forced oscillation technique, that permits to measure the dynamic stability parameters in a relatively simple way. The development of this procedure is one of the results of an experimental research program (see also [1]–[4]) of the Aerospace Engineering Department of the Politecnico di Torino.

1.1. Nomenclature

a_{Mj}	Balance calibration matrix
$C_{l\beta}\sin\alpha$	Roll stiffness coefficient
$C_{lp}+C_{l\beta}\sin\alpha$	Roll-damping coefficient
$C_{m\alpha}$	Pitch stiffness coefficient
$C_{mq}+C_{m\dot{\alpha}}$	Pitch-damping coefficient
$E(t)$	Balance output voltage
$E_{\mathrm{IN}}(t)$	In-phase voltage component
$\overline{E_{\mathrm{IN}}}$	Amplitude of the in-phase voltage component
$E_{\mathrm{OUT}}(t)$	Out-of-phase voltage component
$\overline{E_{\mathrm{OUT}}}$	Amplitude of the out-of-phase voltag component
IN	In-phase component (subscript)
j	Balance output index
K	Reduced oscillation frequency ($\omega l/2V$
l	Reference length
Ma	Mach number
$M(t)$	Driving torque
$M_{\mathrm{aer}}(t)$	Aerodynamic pitching moment (bod
M_0	Static pitching moment
M_α	Static pitching moment derivative
$M_{\dot{\alpha}}$	Dynamic pitching moment derivativ
M_q	Dynamic pitching moment derivativ
OUT	Out-of-phase component (subscript)
q	Pitching angular velocity
S	Model wing surface
S_{WT}	Wind tunnel cross-section
Re	Reynolds number
t	Time
T	Wind-off condition (superscript)
W	Wind-on condition (superscript)
X, Y, Z	Body-fixed axes (origin at mass cent
α	Angle of attack
α_m	Mean angle of attack
α_0	Oscillation amplitude in pitch
β	Angle of sideslip
γ	Crank rotation angle
δ	Oscillation frequency error

$\Delta\alpha$	Primary oscillation in pitch
$\Delta(\gamma)$	Oscillation frequency correction
θ	Oscillation amplitude in pitch experiments
σ	Measurement uncertainty (percentage)
ϕ	Roll angle
ϕ_0	Oscillation amplitude in roll
ω	Oscillation frequency

Some symbols are not listed above as they are included in figures.

2. TEST PROCEDURE AND DATA REDUCTION

The test procedure is based on the measurement of the external loads acting on the model oscillating with respect to its centre of gravity. This primary motion must be harmonic, so that, within the assumption that the system behaviour is linear, the aerodynamic loads can be described as a function of time through their vectorial formulation. Small oscillation amplitudes and frequencies are required for the application of this small perturbation analysis [5].

These considerations underline the importance of the primary motion control, as any distorsion of the oscillation could produce a failure in the measurement technique, introducing a considerable error in the data reduction process.

The forced oscillation experiments can best be explained by describing a typical test.

With the model statically set at an angle of attack α_m (mean value), the tunnel air speed is brought up to the desired velocity. After that, the model is oscillated at a fixed frequency and amplitude, and the aerodynamic forces and moments are measured by the data-acquisition system (wind-on condition). The same experiment is repeated without turning on the wind tunnel (wind-off condition) in order to subtract the effect of inertial loads, mechanical stiffness, mechanical damping and still-air damping, even if the last contribution is generally negligible [6].

All these effects are related to the in-phase and out-of-phase components of the driving forces, measured by the force transducer. This can be explained considering the vectorial representation of the equilibrium of the external loads on the model: the stiffness and the inertial loads have the same vectorial direction of the displacement vector (in-phase), while the direction of the damping contribution is orthogonal (out-of-phase).

Finally, the differences between the wind-on and the wind-off measurements, for the in-phase and out-of-phase components, give respectively the values of the aerodynamic stiffness and damping force contributions.

This method is effective for small amplitude oscillations about one of the three reference body axes: X (roll), Y (pitch) and Z (yaw). In particular the output of the strain-gauge balance, for the oscillation in pitch, is expressed as:

$$\vec{M}(t) = \sum_{j=1}^{n} a_{Mj}\vec{E}_j(t) = \sum_{j=1}^{n} a_{Mj}[\vec{E}_{\mathrm{IN}}(t) + \vec{E}_{\mathrm{OUT}}(t)]_j \tag{1}$$

where n is the dimension of the calibration matrix. The two voltage components can be written as:

$$\begin{aligned} E_{\mathrm{IN}}(t) &= \overline{E_{\mathrm{IN}}}\cos(\omega t), \\ E_{\mathrm{OUT}}(t) &= \overline{E_{\mathrm{OUT}}}\sin(\omega t). \end{aligned} \tag{2}$$

These equations are verified only if the primary oscillatory motion (cosine wave) generates a harmonic reaction on the force transducer that supports the model. Therefore, the two terms $\overline{E_{\mathrm{IN}}}$ and $\overline{E_{\mathrm{OUT}}}$ can be obtained for each j-component, in accordance with the expression of the first-order terms of Fourier harmonic series:

$$\begin{aligned} \overline{E_{\mathrm{IN}}} &= \frac{1}{\pi}\int_0^{2\pi} E(t)\cos(\omega t)\,\mathrm{d}(\omega t), \\ \overline{E_{\mathrm{OUT}}} &= \frac{1}{\pi}\int_0^{2\pi} E(t)\sin(\omega t)\,\mathrm{d}(\omega t). \end{aligned} \tag{3}$$

If small perturbation analysis is supposed to apply, the aerodynamic pitching moment M_{aer} can be expressed as a function of stability parameters and motion variables:

$$M_{\mathrm{aer}}(t) = M_0 + M_\alpha \Delta\alpha + M_{\dot\alpha}\Delta\dot\alpha + M_q q. \tag{4}$$

The oscillatory motion in pitch produces the following kinematical relations (note that the rotation axis is the Y body axis):

$$\begin{aligned} \Delta\alpha &= \alpha_0\cos(\omega t), \\ \Delta\dot\alpha &= -\omega\alpha_0\sin(\omega t), \\ q &= \Delta\dot\alpha. \end{aligned} \tag{5}$$

Considering the dynamic equilibrium of the oscillating model in the two test conditions (wind on and wind off), it is possible to find the expressions of stability derivatives:

$$\begin{aligned} M_\alpha &= \frac{1}{\alpha_0}\cdot\sum_{j=1}^{n} a_{Mj}[\overline{E_{\mathrm{IN}}^{\mathrm{T}}} - \overline{E_{\mathrm{IN}}^{\mathrm{W}}}]_j \\ M_q + M_{\dot\alpha} &= \frac{1}{\omega\alpha_0}\cdot\sum_{j=1}^{n} a_{Mj}[\overline{E_{\mathrm{OUT}}^{\mathrm{T}}} - \overline{E_{\mathrm{OUT}}^{\mathrm{W}}}]_j \end{aligned} \tag{6}$$

Notice that, when performing this kind of oscillatory tests, the effects of q and $\dot\alpha$ cannot be separated.

Similar considerations on the data reduction procedure can be repeated for the rolling and yawing experiments.

3. THE EXPERIMENTAL APPARATUS

A specific servo-mechanical unit was designed in order to perform static tests on the aircraft model and to generate the small amplitude harmonic motion in the three rotational degrees of freedom separately, required for the application of the direct forced oscillation technique.

The facility was adapted at Politecnico di Torino to the

D3M low-speed wind tunnel. A vertical strut supports the model, that is connected to the strain-gauge balance by an internal leverage, that links the fuselage with an oscillating vertical rod. The leverage configuration can be easily changed according to the different primary oscillations (pitch, roll). When yaw oscillations are performed, a different strut is used and the model is suspended in a 90° rotated position.

The harmonic motion of the model is excited by a driving unit that is placed under the floor of the wind tunnel test section; it is powered by a DC motor and is linked to the main rod which supports the fuselage by a gearbox connected to an adjustable flywheel. Setting the flywheel radius, it is possible to modify the oscillation amplitude of the model (maximum $\alpha_0 = \pm 3.5°$). The oscillation frequency of the model (the upper limit is 5 Hz) is set by the rotation speed of the DC motor.

The large angular motion that is necessary to modify the angles of attack and sideslip of the model, both in static and dynamic tests, is generated by two different step motors: the former, translating vertically the dynamic motion unit, acts on the rod and it changes the main leverages position that determines the angle of attack of the model (α ranges from $-7°$ to $+60°$); the latter rotates the vertical strut, modifying the angle of sideslip (β ranges from $-15°$ to $+15°$).

An electronic control unit (ServoData) is interfaced to the mechanical apparatus by a complete set of sensors, transducers and micro-switches [7]. The power drivers (pulse width modulators) of the actuators are electrically connected to ServoData. The control unit is linked to the control PC by a special electronic device (interface board), and the synchronization with the data acquisition computer is possible (handshake or triggering).

The position of the model and its oscillation is controlled directly by an open loop control sequence and the software is designed in order to correct the distorsions on the cosine wave, induced by the different geometrical configurations of the support and of the leverage [8]. This correction algorithm is presented in the following section.

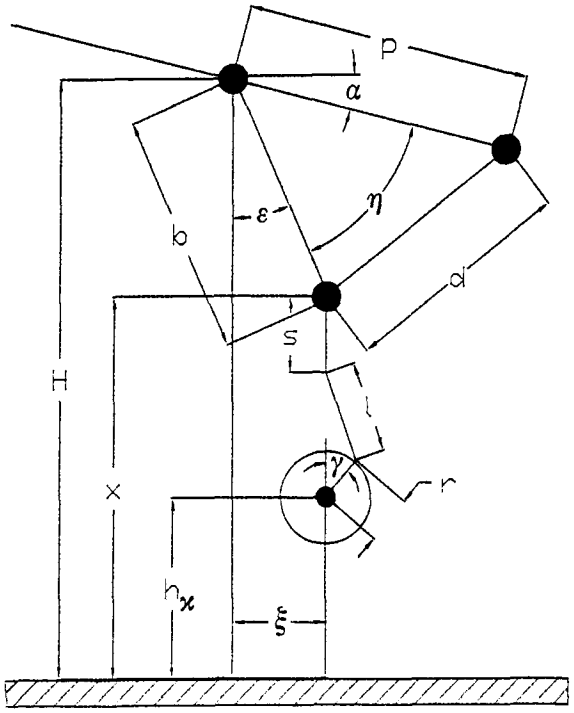

Fig. 1. Layout for pitch and yaw oscillation.

4. THE CONTROL ALGORITHM

4.1. The Oscillation in Pitch

This section describes the calculation of the angular speed $d\gamma/dt$ required for the primary motor control, so that the angle of attack of the model, α, is represented by the following oscillatory function:

$$\alpha(t) = \alpha_m - \alpha_0 \cos(\omega t). \tag{7}$$

As the transmission of the motion (see Figure 1) occurs with the same geometrical configuration for the oscillation both in pitch and in yaw, the angular speed correction is the same.

The angular speed is calculated by determining the function linking the rotational speed of the primary DC motor to the rotation angle itself (γ). Therefore it is necessary to tabulate the speed $d\gamma/dt$ as a function of the angle γ: for each value of γ, measured by an encoder mechanically linked to the primary DC motor, a value of speed to impress to the above-mentioned motor is found. The table is scanned continuously, in order to carry out the correction step by step. The frequency with which the motor speed is updated is proportional to the encoder status conditions (256 times per revolution).

The link between the motion and the mechanical apparatus is expressed by the following equations:

$$\eta(x) = \arccos \frac{p^2 + b^2(x) - d^2}{2pb(x)}, \tag{8}$$

$$\varepsilon(x) = \arctan \frac{\xi}{H - x}, \tag{9}$$

$$\alpha(x) = \frac{\pi}{2} - \eta(x) - \varepsilon(x). \tag{10}$$

By defining $\lambda = r/l$ and looking at the geometry of the rod–crank system, we can easily correlate the variable x and the crank angle γ:

$$x(\gamma) = h_x + s + r\cos\gamma + l\sqrt{1 - \lambda^2 \sin^2\gamma}. \tag{11}$$

In order to evaluate the speed $d\gamma/dt$ required for the control, it is possible to obtain:

$$\frac{d\alpha}{dt}(\gamma) = \frac{d\alpha}{d\gamma}(\gamma) \cdot \frac{d\gamma}{dt}(\gamma) = \frac{d\alpha}{dx}(x(\gamma)) \cdot \frac{dx}{d\gamma}(\gamma) \cdot \frac{d\gamma}{dt}(\gamma). \tag{12}$$

Hence:

$$\frac{d\gamma}{dt}(\gamma) = \frac{d\alpha(\gamma)}{dt} \Big/ \left(\frac{d\alpha(x(\gamma))}{dx} \cdot \frac{dx(\gamma)}{d\gamma} \right). \tag{13}$$

The derivatives $(d\alpha/dx)(x)$ and $(dx/d\gamma)(\gamma)$ in the denominator of the second term in the previous equation can be easily obtained by differentiating (10) and (11). Solving (7) with respect to the variable t, we obtain:

$$t = \frac{1}{\omega} \cdot \arccos \frac{\alpha_m - \alpha}{\alpha_0} \tag{14}$$

which can be introduced in $d\alpha(t)/dt$ in order to eliminate the time dependence.

The mean angle of attack α_m and the amplitude of oscillation α_0 are geometrically related to the variables r and h_x. These quantities are evaluated from (10) and (11), so that the highest and lowest values of the angle α are found, in correspondence with the lowest and highest values of the variable x. Therefore, we can obtain α_0 and α_m.

The calculation of the values associated to the vector $\{d\gamma/dt, \gamma\}$ is carried out by relating each encoder status to the corresponding value of the angle γ in the range $[0, 2\pi[$. The substitution of the last value of γ into (11) determines the solution of (10); on the other hand, this equation defines completely (9) by means of α_0, α_m and (14). The substitution of γ into $d\alpha(x)/dx$ and (11), and finally into $dx(\gamma)/d\gamma$, gives the possibility of finding the last two unknown terms of (13).

The mathematical expression of $d\gamma(\gamma)/dt$ can be divided in two contributions: the first one (ω) is not dependent from γ, and the second one is a function of γ, the correction $\Delta(\gamma)$:

$$\frac{d\gamma}{dt}(\gamma) = \omega + \Delta(\gamma). \tag{15}$$

Two examples of the function $\Delta(\gamma)$ are illustrated in Figure 2.

4.2. The Oscillation in Roll

The mechanical layout used to generate the motion for the roll configuration is sketched in Figure 3. Even though it is slightly different from the one described previously, most of the equations developed can be still applied here. The angle ϕ is assumed to follow an oscillatory motion:

$$\phi(t) = \phi_0 \cos \omega t. \tag{16}$$

The link between this variable and the crank angle γ must be found. From Figure 3 it is possible to obtain that:

$$y(t) = H - p \sin \rho(t) \tag{17}$$

where $\rho(t)$ has the same meaning of the angle $\alpha(t)$ described in the previous section, when a reference is made to the equations of the last part.

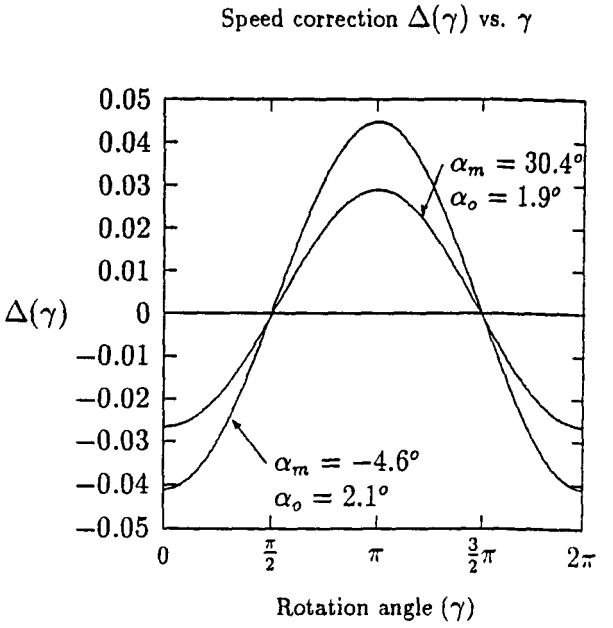

Fig. 2. Speed corrections for pitch oscillation in two different configurations at $\omega = 1$ rad/s.

On the other hand, the angle $\rho(t)$ can be divided into a constant part depending on the model mean angle of attack (α_m) and into another one, time dependent, deriving from the oscillation of the model itself. If we replace the equation $\rho(t) = \alpha_m - \Delta\rho(t)$ into the previous relation, considering that it is possible to carry out the approximation $\cos \Delta\rho(t) \simeq 1$ as the angle $\Delta\rho$ is small, the following relation is found:

$$y(t) = H - p \sin \alpha_m + p \cos \alpha_m \sin \Delta\rho(t). \tag{18}$$

Defining $y_m = H - p \sin \alpha_m$ and $\Delta y(t) = p \cos \alpha_m \sin \Delta\rho(t)$, and looking at Figure 3, a second equation for $\Delta y(t)$ is found:

$$\Delta y(t) = b_r \sin \phi(t) = p \cos \alpha_m \sin \Delta\rho(t). \tag{19}$$

The value of ϕ_0 is obtained in accordance with the procedure discussed in the previous section. This angular displacement is linked to the parameters r and h_x: as shown in Figure 3, the highest value of ϕ is obtained with the highest value of x, that generates the lowest angle $\rho_{\min} = \alpha_m - \Delta\rho_{\min}$. From (19) it is possible to find:

$$\phi_0 = \arcsin \left[\frac{p \cos \alpha_m}{b_r} \sin \Delta\rho_{\min} \right]. \tag{20}$$

As (16) was totally defined, the same method adopted in the section above can be used, in order to determine the table $\{d\gamma/dt, \gamma\}$:

$$\frac{d\phi}{dt}(\gamma) = \frac{d\phi}{d\rho}(\rho(\gamma)) \cdot \frac{d\rho}{dt}(\gamma). \tag{21}$$

The term $d\phi(\rho(\gamma))/d\rho$ is found making $\phi(t)$ explicit from (19) and deriving it with respect to ρ. On the other hand, differentiating (16) with respect to time, a formulation for

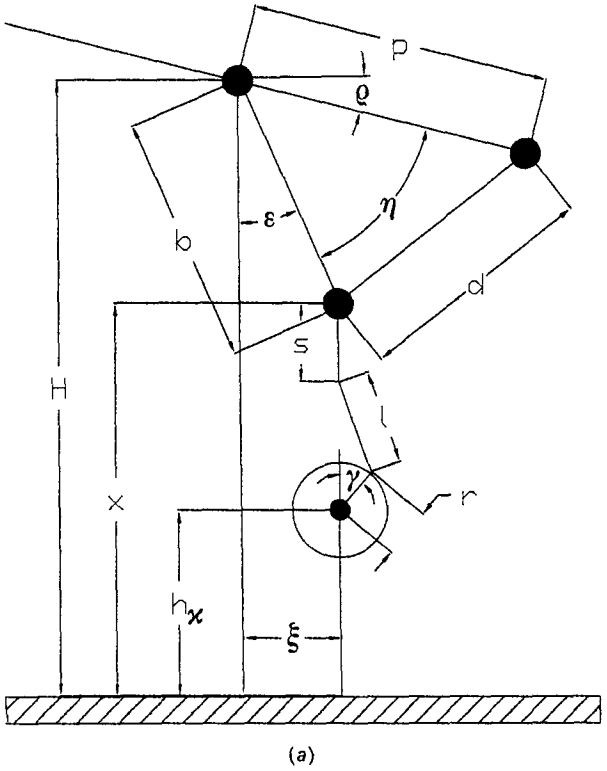

(a)

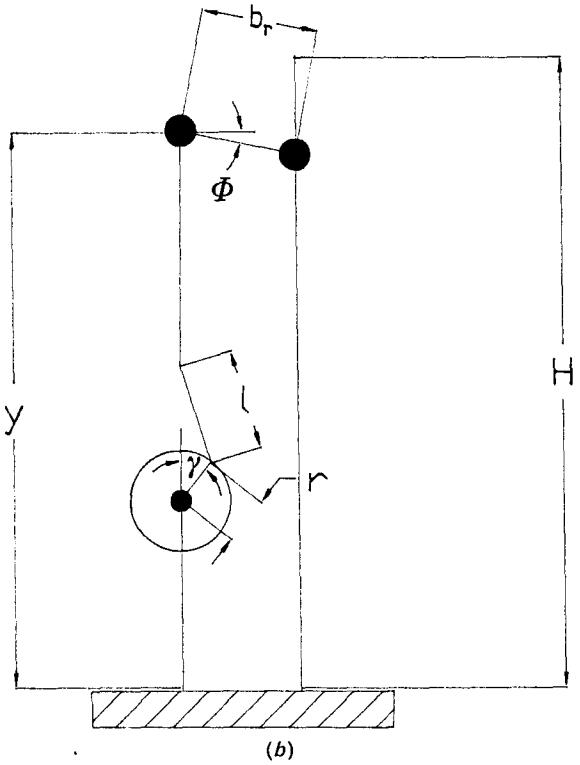

(b)

Fig. 3. Layout for roll oscillation.

$d\phi/dt$ is obtained, where t must be replaced by

$$t = \frac{1}{\omega} \cdot \arccos \frac{\phi(\gamma)}{\phi_0}. \tag{22}$$

From relation (21) $d\rho(\gamma)/dt$ can be found, which is related to $d\gamma(\gamma)/dt$ using Equation (12).

In this case, as well, the trend of the correction is shown at different model mean angles of attack (see Figure 4).

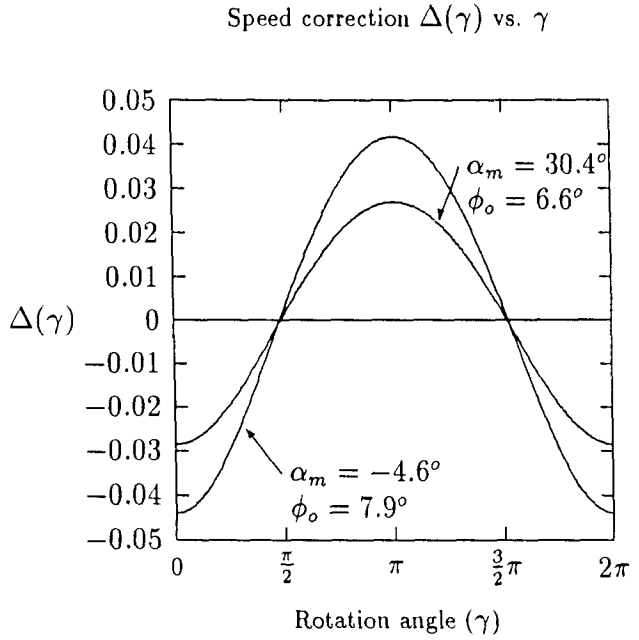

Fig. 4. Speed corrections for roll oscillation in two different configurations at $\omega = 1$ rad/s.

4.3. The Verification of the Control Algorithm

In order to verify the reliability of the speed corrections, the motion of the primary DC motor was simulated with and without correction. The angle α (and the angle ϕ respectively), described as a function of angle γ, has been compared in each case with an ideal trend like (7) (and like (16) respectively). The time t, present in Equations (7) and (16), is related to the angle γ by means of two equations:

$$t = \frac{\gamma}{\omega} \tag{23}$$

with no correction, and

$$t = \int_0^t \frac{dt}{d\gamma} \cdot d\gamma = \int_0^t \frac{1}{\Delta(\gamma) + \omega} \cdot d\gamma \tag{24}$$

with correction. These relations identify some pairs $\{\gamma, t\}$ which, through (10), (11) and (7) (and (10), (11), (19) and (16) respectively) allow us to identify the following functions:

$$\delta(t) = \alpha(t) - [\alpha_m - \alpha_0 \cos \omega t] \tag{25}$$

in the case of pitch and yaw oscillations and

$$\delta(t) = \phi(t) - [\phi_0 \cos \omega t] \tag{26}$$

for what concerns roll oscillations.

These functions represent the error in the model trajectory compared with the ideal one. Such errors, in the absence of correction, are shown in Figures 5 and 6 for each mode of oscillation. When the correction is activated, the function $\delta(t)$ is identically null, at least, up to the seventh decimal digit along the whole interval $[0, 2\pi[$ of the variation of γ.

Furthermore, the effect of correction was investigated

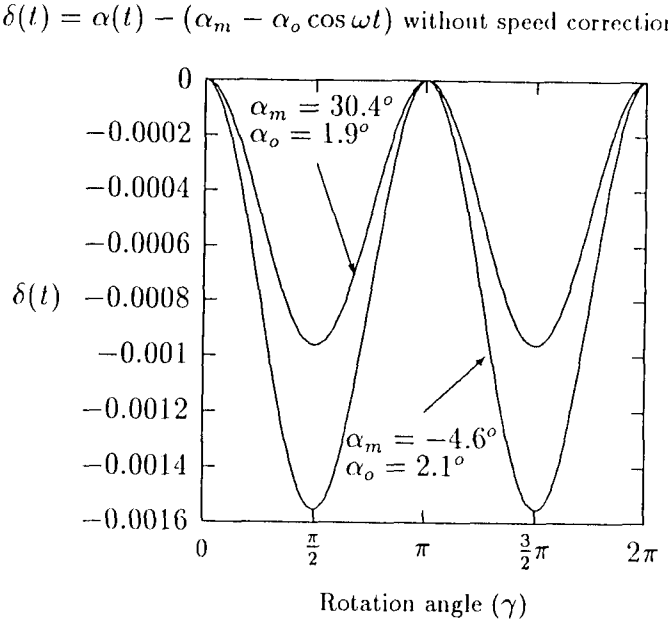

Fig. 5. Oscillation error for pitch oscillation at $\omega = 1$ rad/s.

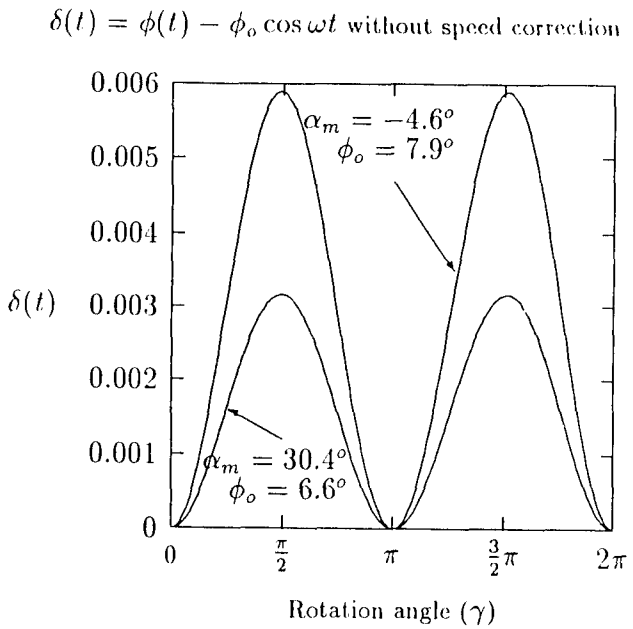

Fig. 6. Oscillation error for roll oscillation at $\omega = 1$ rad/s.

during the calibration of the moving rig, and the experimental results are in good agreement with the numerical simulations presented (see also [8]).

5. THE EXPERIMENTAL STABILITY PARAMETERS

The primary sources for aircraft dynamic stability derivatives are the forced oscillation wind tunnel tests. These experiments provide the non-dimensional derivatives about the three rotational body axes in a form that is a combination of rate and acceleration contributions.

Generally, these results are substantially influenced by the interference of the model support, which can be hardly evaluated. The comprehension of this last aerodynamic interaction is critical, as different factors depending on the support affect the measurement [9] of the experimental stability parameters: the test section flow angularity (i.e. the flow non-uniformity generated by the support), the aerodynamic support interference (i.e. the influence on the flow field around the model of disturbances communicated upstream from the support) and, finally, the support motion.

Actually, the only way to verify the effect of these support interferences is a comparison of the results obtained with similar models using different rigs (see Figure 10).

The uncertainty of the experimental measurements is further complicated by the interactions between the control system and the data acquisition unit (i.e. the generation of electronic noise on the output signals or the distorsion of the primary motion). These effects should be evaluated and reduced to a minimum [8].

Finally, the influence of reduced frequency and oscillation amplitude on these stability parameters must be carefully investigated.

Therefore, with the aim of giving a contribution to the understanding of these experimental problems, a set of wind tunnel tests was performed on a standard calibration model (the Standard Dynamics Model) at Politecnico di Torino and the above-presented apparatus was adapted to the D3M low-speed wind tunnel belonging to the Aeronautical Laboratory of the Aerospace Engineering Department. A short description of the experimental setup follows.

The model dimensions are: length 943 mm, wing span 609 mm, mean aerodynamic chord 220 mm and wing area 0.117 m^2. This model has a typical fighter aircraft configuration [10] and the wing has a trapezoidal planform with a 40° sweep angle and sharpended leading edge. The fuselage is symmetric with an ogival forebody (see Figure 7).

The centre of gravity of the oscillating system is at 35% of the mean aerodynamic chord and, as the vertical support must be linked to the internal leverage connected to the balance, a rectangular milling is present in the ventral part of the fuselage. Static pressure measurements demonstrated that the influence of the support on this part of the model surface is small. Model wake blockage is negligible for $\alpha < 30°$ (the ratio $S/S_{WT} = 0.016$ is quite low [11]).

The experiments were performed at $Ma = 0.12$ and $Re = 530\,000$ (based on the mean aerodynamic chord). It is important to remark that this model has a low sensitivity to this last parameter, due to the sharpened leading edge profile. Furthermore, the increase of Mach number affects only marginally the stability parameters of the calibration model in the subsonic range [12], [13].

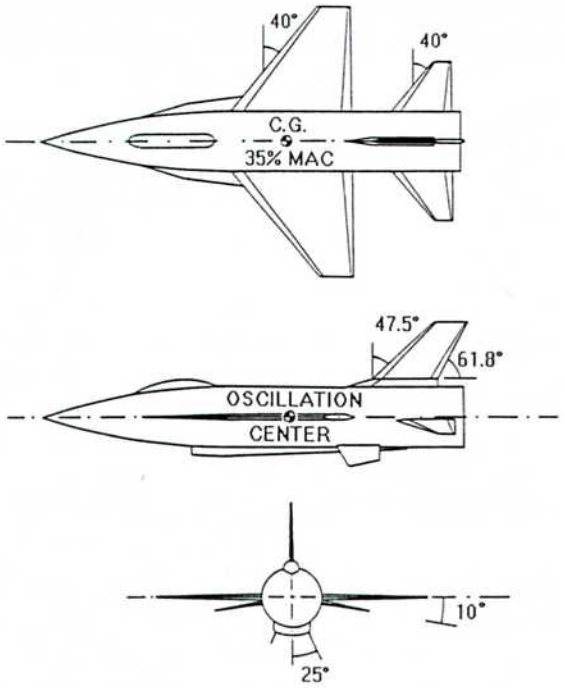

Fig. 7. The standard dynamics model.

The main interest of the experimental programme was the analysis of the behaviour of the stability parameters as a function of angle of attack, reduced frequency and oscillation amplitude. Some of the results of this investigation are discussed in this paper.

The trend of $C_{m\alpha}$ is presented in Figures 8 and 9. For $\alpha > 18°$, where the wing-stall occurs, the effects of oscillation frequency and amplitude become evident. A remarkable deviation from the $K = 0$ curve (obtained from static data) is detected for the coefficients evaluated in oscillatory conditions.

The damping derivative $(C_{mq} + C_{m\dot{\alpha}})$ is stable (i.e. negative) in the α-range considered. Nevertheless, some

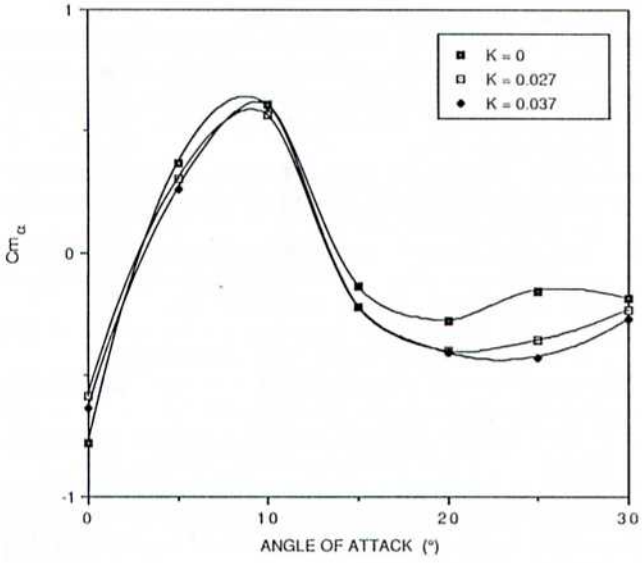

Fig. 8. The effect of oscillation frequency on $C_{m\alpha}$ at $Ma = 0.12$ ($\theta = \pm 1.5°$).

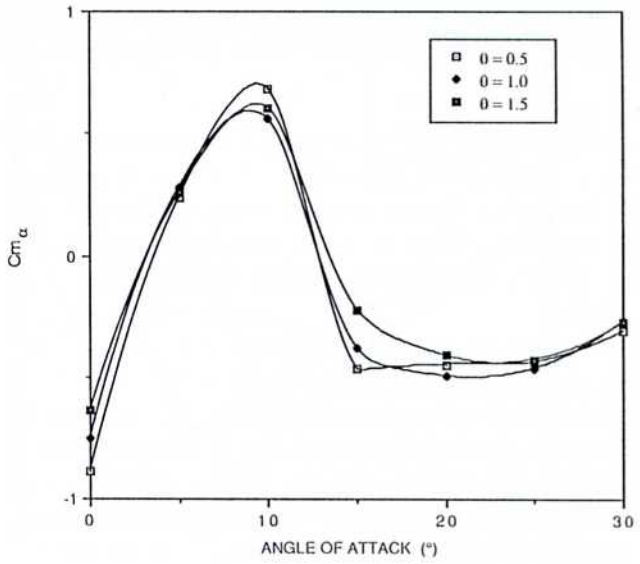

Fig. 9. The effect of oscillation amplitude on $C_{m\alpha}$ at $Ma = 0.12$ ($K = 0.037$).

important remarks are required. The increments of this stability parameter due to the variation of the reduced frequency and the oscillation amplitude were evaluated. Their trends are non-linear functions of the test parameters (α_m, K, θ) and their magnitude is comparable with the measurement uncertainty of $(C_{mq} + C_{m\dot{\alpha}})$: $\sigma = \pm 5.5\%$ for $\alpha_m < 30°$.

This considerable margin of uncertainty is confirmed for the measurements of $(C_{mq} + C_{m\dot{\alpha}})$ in reference [10], where $\sigma = \pm 4\%$ at low angle of attack and $\sigma = \pm 10\%$ at higher α_m.

In Figure 10 the trend of this damping derivative is compared with the results obtained by N.R.C. [10] and by F.F.A. [13]. These tests were performed at higher subsonic air speeds on models of smaller size, using a rear sting support. Unfortunately, these data were evaluated with different reduced frequencies and oscillation amplitudes.

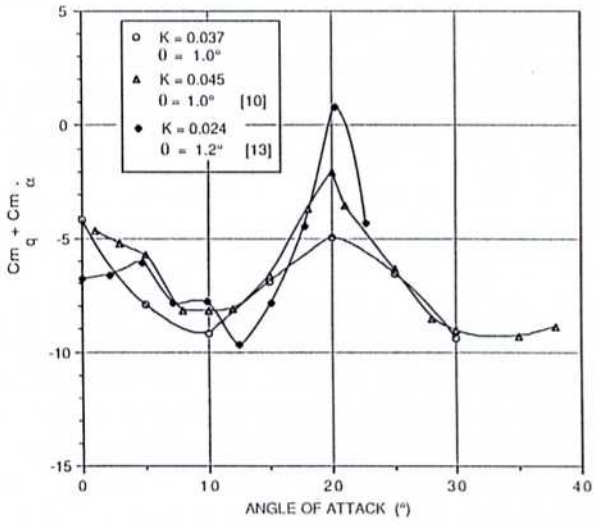

Fig. 10. The damping derivative $(C_{mq} + C_{m\dot{\alpha}})$ for the standard dynamics model obtained in different test conditions.

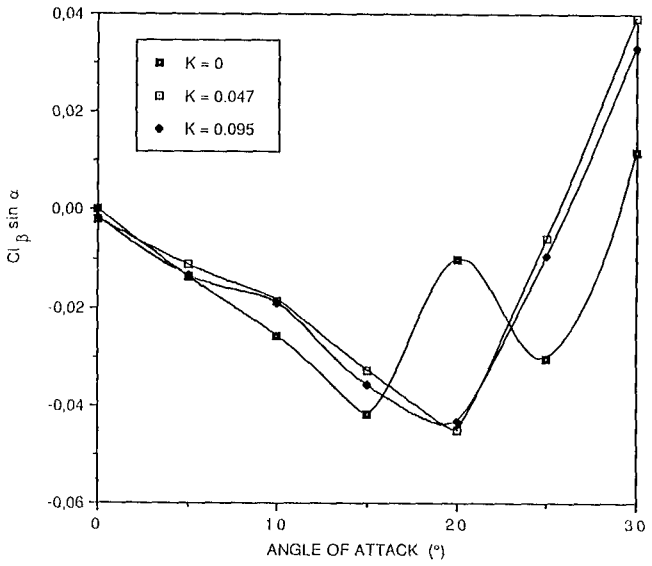

Fig. 11. The effect of oscillation frequency on $C_{l\beta} \sin \alpha$ at $Ma = 0.12$ ($\phi_0 = \pm 2.1°$).

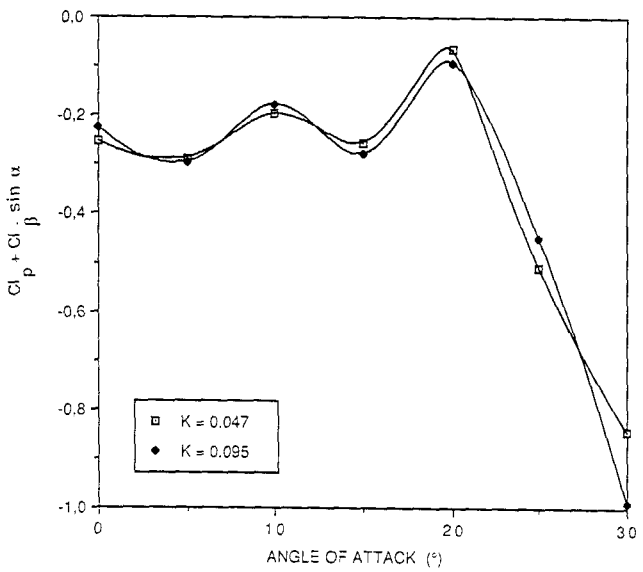

Fig. 12. The effect of oscillation frequency on $(C_{l_p} + C_{l\dot{\beta}} \sin \alpha)$ at $Ma = 0.12$ ($\phi_0 = \pm 2.1°$).

Hence, only a qualitative comparison with these reference results is possible, taking into account the different test conditions and the considerable measurement uncertainties (an intermediate value of K and a similar value of θ were considered).

The trends are similar, but this comparison confirms the importance of support interference when damping terms in pitch are measured with this experimental technique. Some discrepancies are found even at low angle of attack, where the vertical strut can affect the flow field around the lower part of the fuselage. At wing-stall ($\alpha_m \approx 20°$) the situation is critical, and the three sets of data are consistently different. At higher α_m, in the region where separated flows are predominant, the agreement of the measurements is improved.

The effect of oscillation frequency on roll derivatives has been evaluated (see Figures 11 and 12). The trend of the roll stiffness coefficient $C_{l\beta} \sin \alpha$ confirms that the dynamic data move away from static ones in the α-range beyond the wing-stall.

The effect of oscillation amplitude ($\phi_0 = 1$–$2.1°$) on these dynamic rotary derivatives is not important for the incidence range tested.

6. CONCLUDING REMARKS

The moving rig for the determination of stability parameters, adopted at the Aeronautical Laboratory of Politecnico di Torino was described. The data reduction procedure and the control algorithm were discussed. The experimental results were related to the primary motion frequency and amplitude. A critical comparison of the measurements of the damping derivative $(C_{mq} + C_{m\dot{\alpha}})$, performed in different wind tunnels with different supporting systems, confirmed that the margin of uncertainty for the results obtained at Politecnico di Torino is acceptable.

REFERENCES

1. Cavallari, A., Guglieri, G. and Quagliotti, F., 'Progetto e costruzione di un sistema per la determinazione delle derivate di smorzamento in galleria del vento', *10th AIDAA Congress, Pisa, Italy*, 1989.
2. Cavallari, A., Guglieri, G. and Quagliotti, F., 'Development of a measurement technique for damping derivatives in pitch', *17th ICAS Congress, Stockholm, Sweden*, 1990.
3. Cavallari, A., Guglieri, G. and Quagliotti, F., 'Development of experimental methods for dynamic derivatives measurement in wind tunnels', *International Aerospace Congress, Melbourne, Australia*, 1991.
4. Guglieri, G. and Quagliotti, F., 'Determination of dynamic stability parameters in a low speed wind tunnel', *9th AIAA Applied Aerodynamics Conf., Baltimore, U.S.A.*, 1991.
5. Tobak, M. and Schiff, L. B., 'Aerodynamic mathematical modeling–basic concepts', *AGARD Lecture Series*, No. 114, 1981.
6. Hanff, E.S., 'Direct forced oscillation techniques for the determination of stability derivatives in wind tunnel', *AGARD Lecture Series*, No. 114, 1981.
7. Fusco, F., Guglieri, G. *et al.*, 'ServoData: unitá di controllo ed interfacciamento', TN 43, Politecnico di Torino, Dip. Ing. Aeronautica e Spaziale, Torino, Italy, 1991.
8. Costantin, C., Fusco, F. and Guglieri, G., 'Tecniche di controllo ed acquisizione dati per prove di oscillazione forzata in galleria del vento', *11th AIDAA Congress, Forlí, Italy*, 1991.
9. Beyers, M.E., 'Some recent N.A.E. experiences of support interference in dynamic tests', LTR-UA-83, Ottawa, Canada, 1985.
10. Beyers, M.E., 'Pitch and yaw oscillation experiments on the SDM at Mach 0.6', LTR-UA-76, Ottawa, Canada, 1984.
11. Barbantini, E. *et al.*, 'Blockage corrections at high angle of attack in a wind tunnel', *16th ICAS Congress, Jerusalem, Israel*, 1988.
12. Schmidt, E., 'SDM experiments with the D.F.V.L.R./A.V.A. transonic derivative balance', *AGARD Conference Proceedings*, No. 386, 1985.
13. Torngren, L., 'Dynamic pitch and yaw derivatives of the SDM', FFA TN 1985–05, Sweden, 1985.